

iScience, Volume 27

Supplemental information

**Presenilin-1 in smooth muscle cells facilitates
hypermuscularization in elastin aortopathy**

Junichi Saito, Jui M. Dave, Freddy Duarte Lau, and Daniel M. Greif

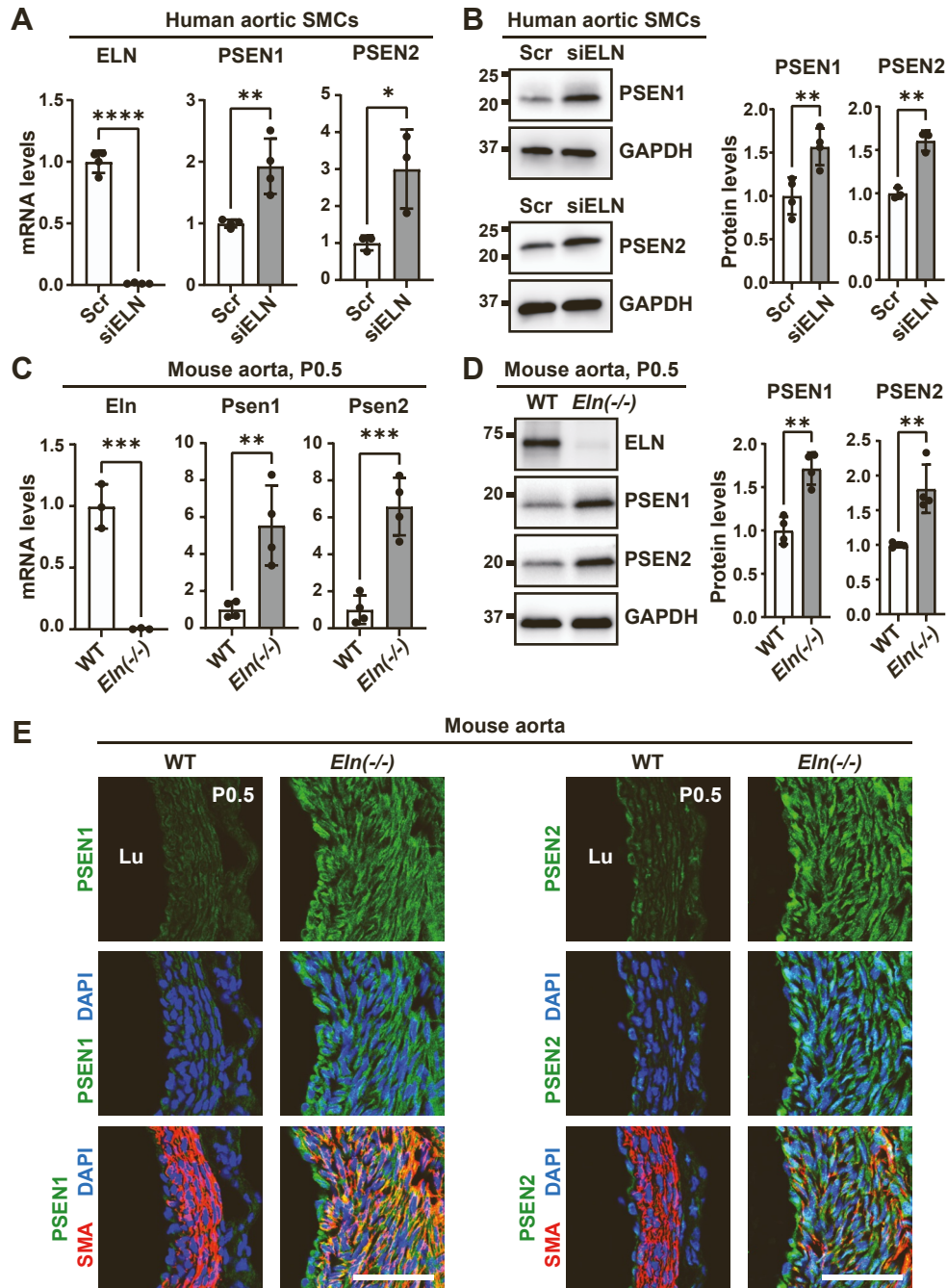


Figure S1. Elastin deficiency upregulates presenilin subunits (PSEN1/2) of gamma-secretase, Related to Figures 1-6. (A-D) Aortic lysates from human aortic SMCs treated with scrambled (Scr) or ELN siRNA (A, B) or from wildtype (WT) or *Eln*^{-/-} mice at P0.5 (C, D) were analyzed. In A and C, histograms depict transcript levels of ELN, PSEN1, and PSEN2 from qRT-PCR relative to 18S rRNA and normalized to Scr or WT. In B and D, Western blot and densitometry of protein bands relative to GAPDH is shown. n=3-4. **P* < 0.05, ***P* < 0.01, ****P* < 0.001, *****P* < 0.0001 by Student's *t* test. Data are presented as mean ± SD. (E) Transverse sections of ascending aorta (cranial position, Fig. S2) of WT or *Eln*^{-/-} mice at P0.5 stained for α-smooth muscle actin (SMA, SMC marker), nuclei (DAPI), and either PSEN1 or PSEN2. n=5 mice. Lu, lumen. Scale bars, 40 μm.

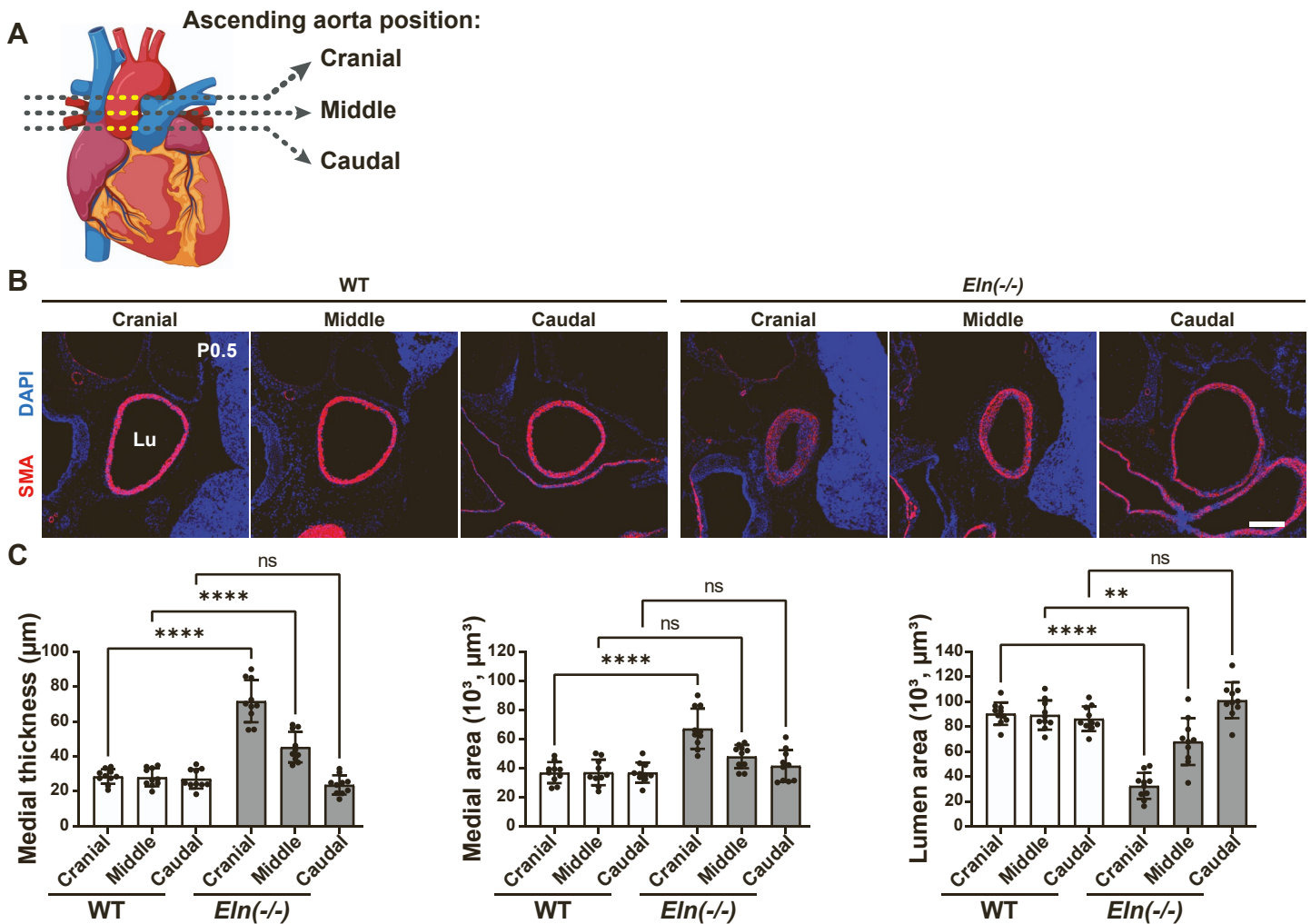


Figure S2. Ascending aorta morphology at different cranio-caudal levels, Related to Figures 1-6. (A) Schematic of the heart and the great vessels. Cranial, middle, and caudal positions of the ascending aorta were analyzed in B and C. Graphical object was created with BioRender. (B) Ascending aortic transverse sections of wildtype (WT) or *Eln*^{-/-} mice at P0.5 stained for SMA and nuclei (DAPI). Lu, lumen. Scale bar, 200 μm. (C) Histograms represent aortic medial wall thickness, medial area and lumen area from images represented by B. n=10 mice. ns, not significant. ** $P < 0.01$, **** $P < 0.0001$ by multifactor ANOVA with Tukey's *post hoc* test. Data are presented as mean ± SD.

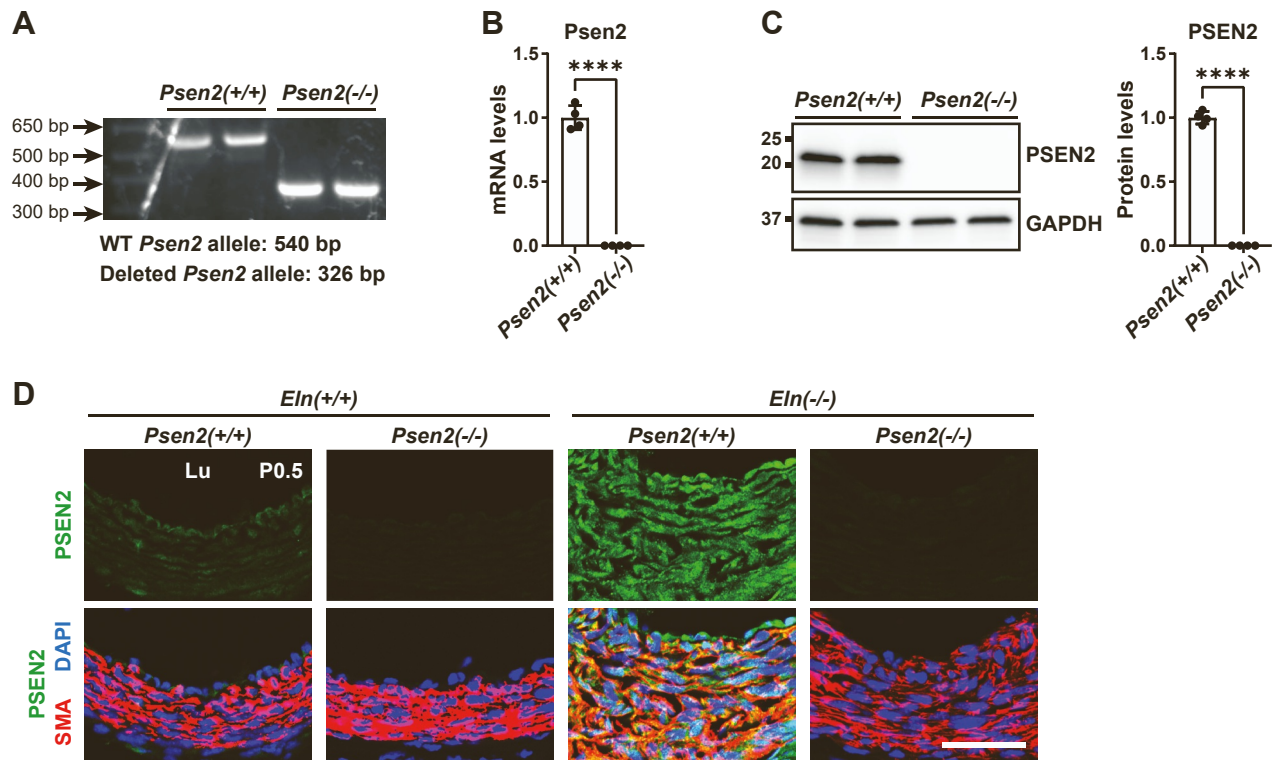


Figure S3. PSEN2 expression in *Psen2* null aorta, Related to Figure 1. (A) Extracted genomic DNA from aortas was subjected to PCR with primers targeting *Psen2*. The 540 bp PCR product represents the WT *Psen2* allele, whereas the 326 bp PCR product represents the deleted *Psen2* allele. n=2 mice. (B) Isolated RNA from aorta was subjected to qRT-PCR. Histogram represents *Psen2* transcript levels relative to 18S. (C) Western blot was performed on protein extracted from the aorta. Densitometry of protein bands relative to GAPDH is shown. In B and C, n=4 mice; **** $P < 0.0001$ by Student's *t* test. Data are presented as mean \pm SD. (D) Transverse sections of the ascending aorta (cranial position, Fig. S2) from pups at P0.5 of indicated genotype were stained for SMA, nuclei (DAPI), and PSEN2. Lu, lumen. Scale bar, 40 μ m.

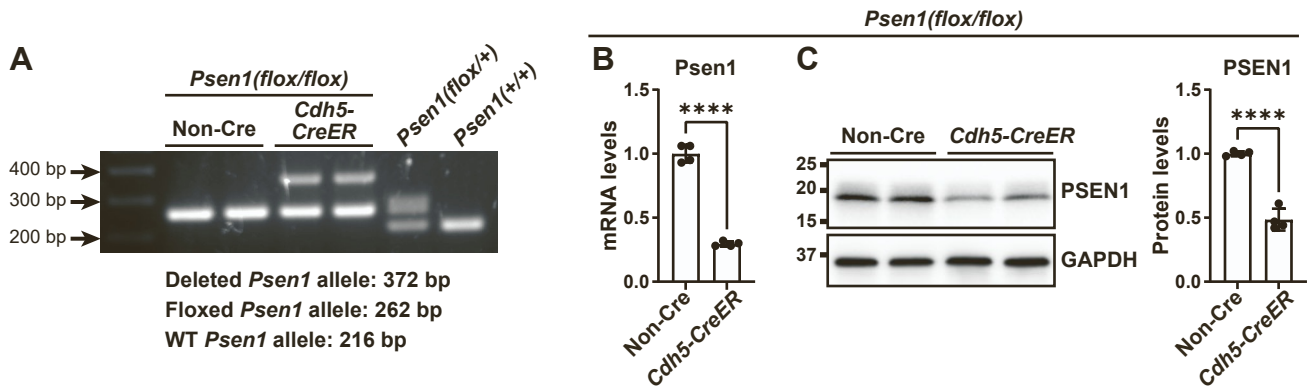


Figure S4. *Psen1* deletion efficiency in ECs of *Cdh5-CreER*^{T2}, *Psen1(flox/flox)* mice, Related to Figure 2. Dams pregnant with *Psen1(flox/flox)* embryos also carrying *Cdh5-CreER*^{T2} or no Cre were injected with tamoxifen at E14.5 and E15.5. ECs were isolated from lungs of pups at P0.5 and subjected to lysis. **(A)** Extracted genomic DNA was subjected to PCR with primers flanking *Psen1*. The 216 bp PCR product represents the WT *Psen1* allele, whereas the 262 bp fragment represents the floxed *Psen1* allele. The 372 bp PCR product represents the deleted *Psen1* allele.¹ **(B)** Isolated RNA was reverse transcribed and subjected to qRT-PCR. Histogram represents *Psen1* transcript levels relative to 18S rRNA. **(C)** Western blot was performed on protein extracted from isolated ECs. Densitometry of protein bands relative to GAPDH is shown. n=4 mice. *****P* < 0.0001 by Student's *t* test. Data are presented as mean ± SD.

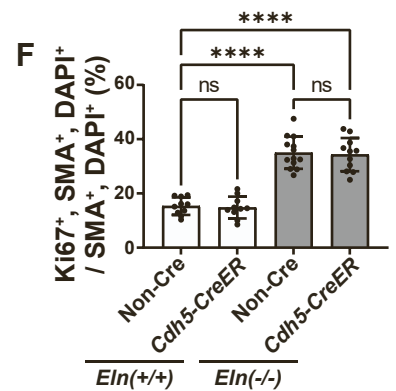
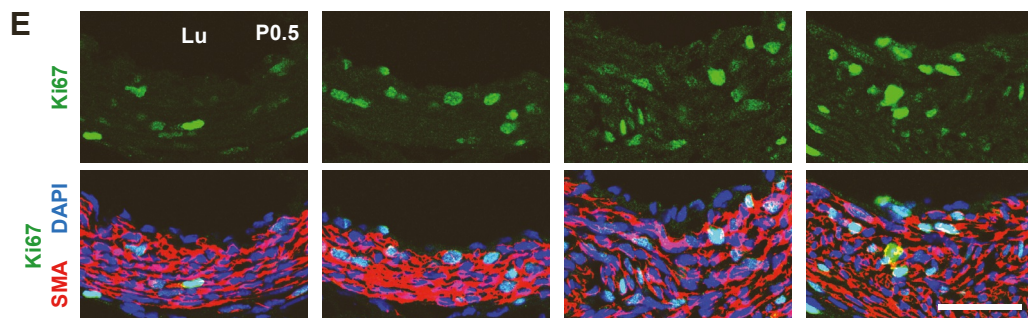
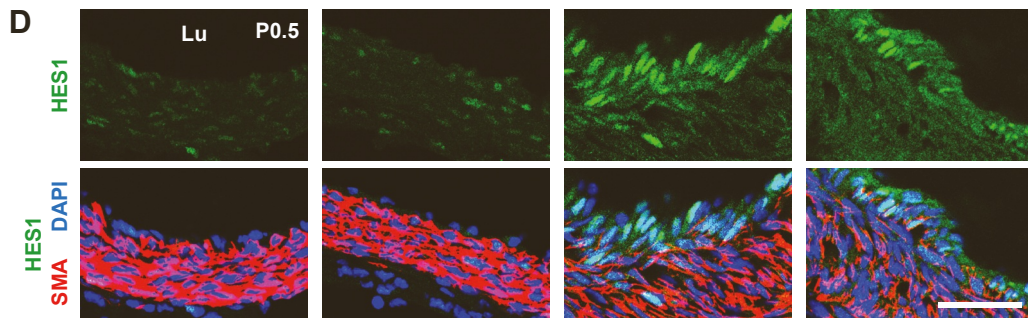
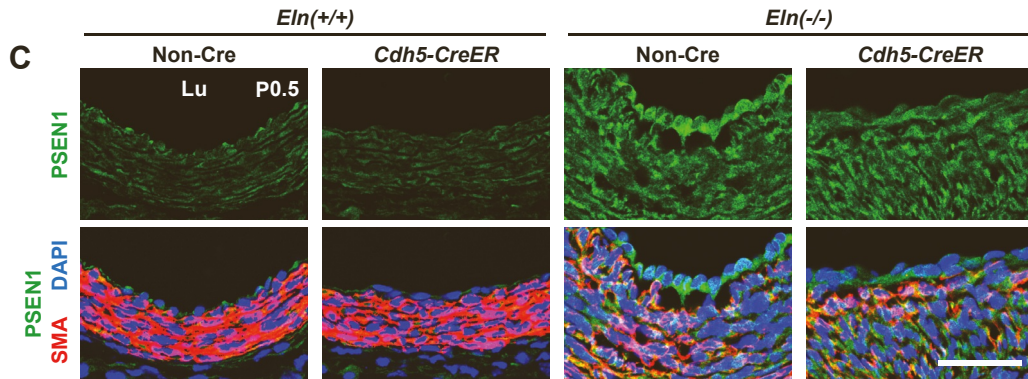
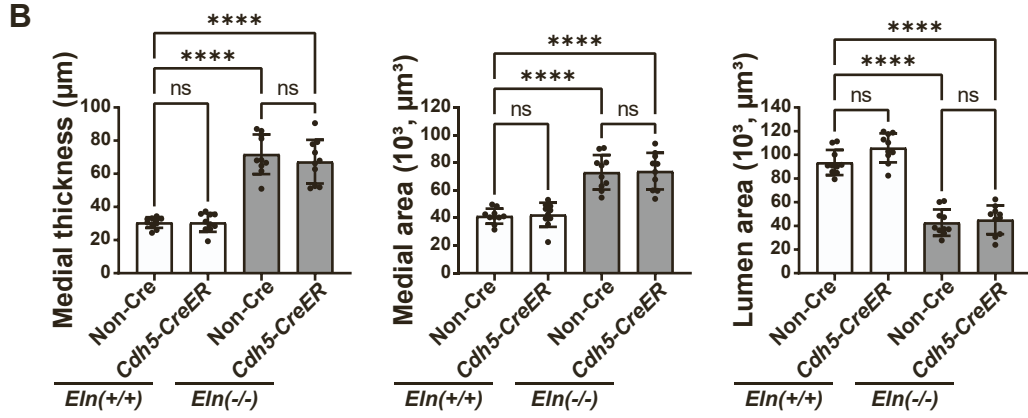
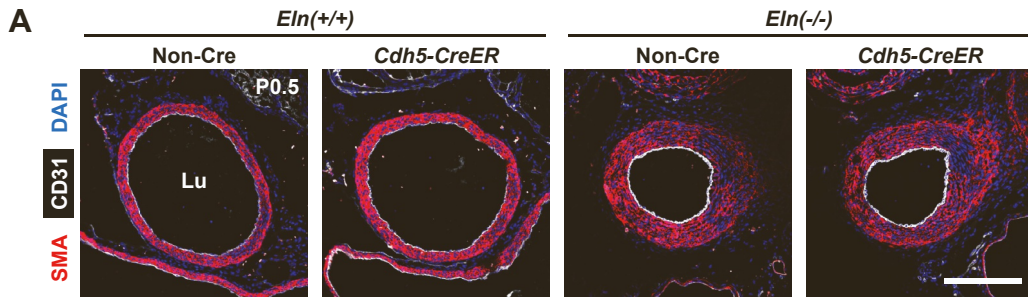


Figure S5. On the *Eln*(-/-) background, EC-specific *Psen1* deletion does not reduce hypermuscularization and stenosis, Related to Figure 2. Transverse sections of the ascending aorta (cranial position, Fig. S2) from pups at P0.5 of indicated genotype were analyzed. **(A)** Sections were stained for SMA, CD31, and nuclei (DAPI). **(B)** Histograms represent aortic medial wall thickness, medial area and lumen area from sections as in **A**. n=10 mice. **(C-E)** Sections were stained for SMA, nuclei (DAPI), and either PSEN1 in **C**, HES1 in **D**, or Ki67 in **E**. **(F)** Histograms represent percent of SMCs that are Ki67⁺ in sections represented by **E**. n=10-13 mice. Lu, lumen. ns, not significant. **** $P < 0.0001$ by multifactor ANOVA with Tukey's *post hoc* test. Data are presented as mean \pm SD. Scale bars, 200 μ m (**A**) and 40 μ m (**C-E**).

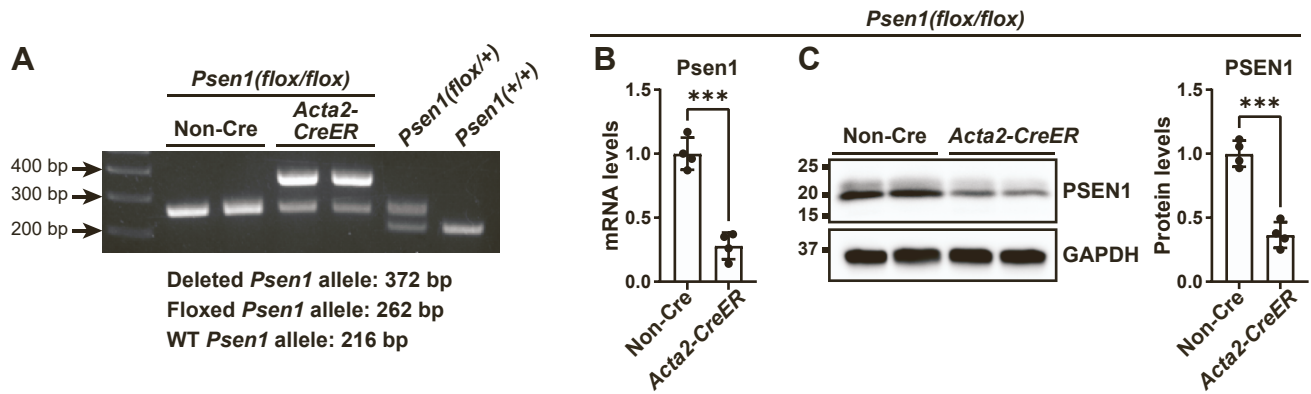


Figure S6. *Psen1* deletion efficiency in aortic SMCs of *Acta2-CreER*^{T2}, *Psen1(flox/flox)* mice, Related to Figure 2. Dams pregnant with *Psen1(flox/flox)* embryos also carrying *Acta2-CreER*^{T2} or no Cre were injected with tamoxifen at E14.5 and E15.5. Aortas were isolated from pups at P0.5 and subjected to lysis after adventitia removal. **(A)** Extracted genomic DNA was subjected to PCR with primers flanking *Psen1*. The 216 bp PCR product represents the WT *Psen1* allele, whereas the 262 bp fragment represents the floxed *Psen1* allele. The 372 bp PCR product represents the deleted *Psen1* allele.¹ **(B)** Isolated RNA was reverse transcribed and subjected to qRT-PCR. Histogram represents *Psen1* transcript levels relative to 18S rRNA. **(C)** Western blot was performed on protein extracted from the aorta. Densitometry of protein bands relative to GAPDH is shown. n=4 mice. ****P* < 0.001 by Student's *t* test. Data are presented as mean ± SD.

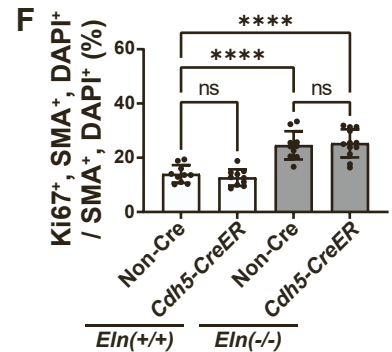
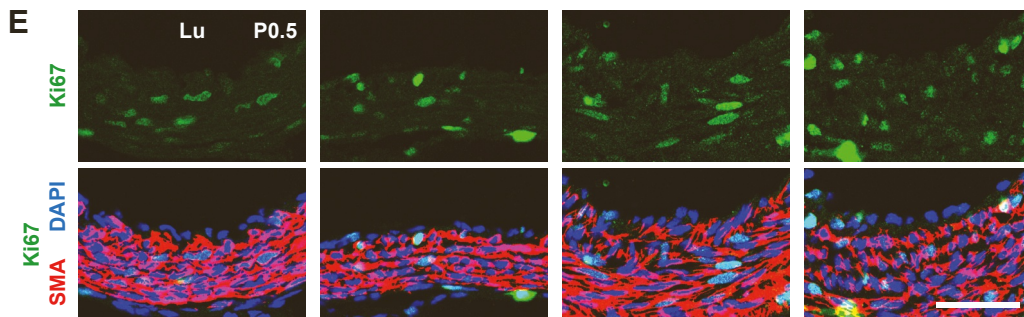
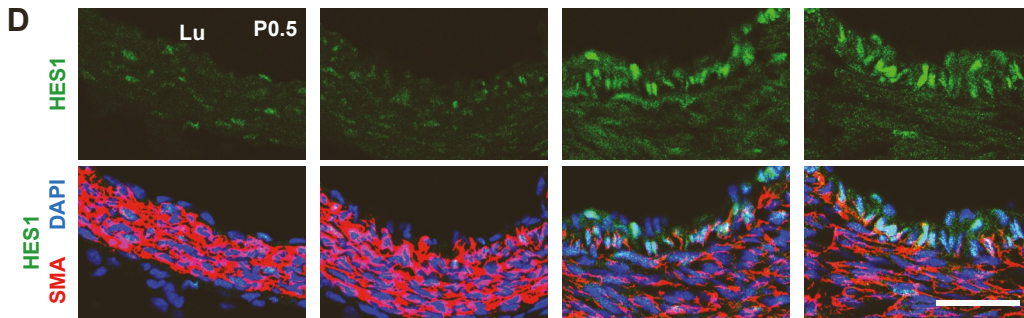
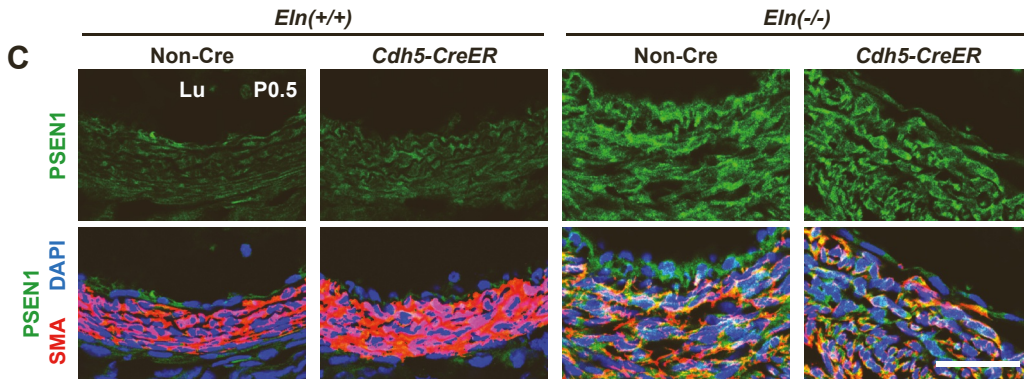
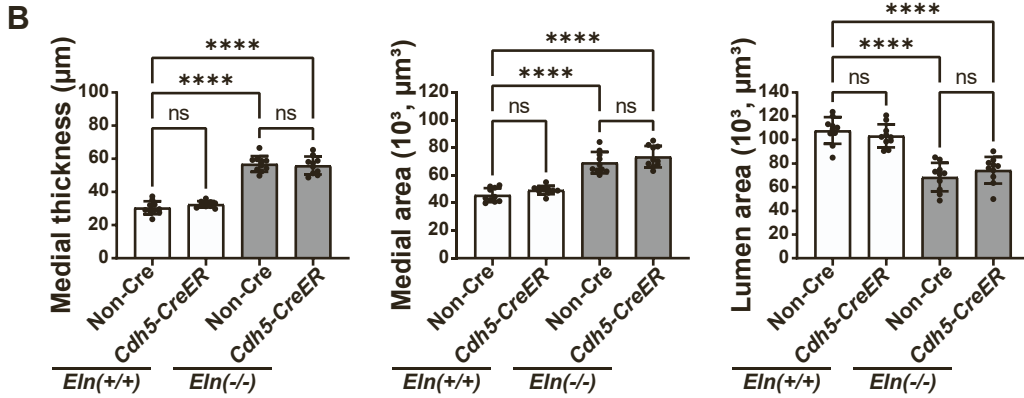
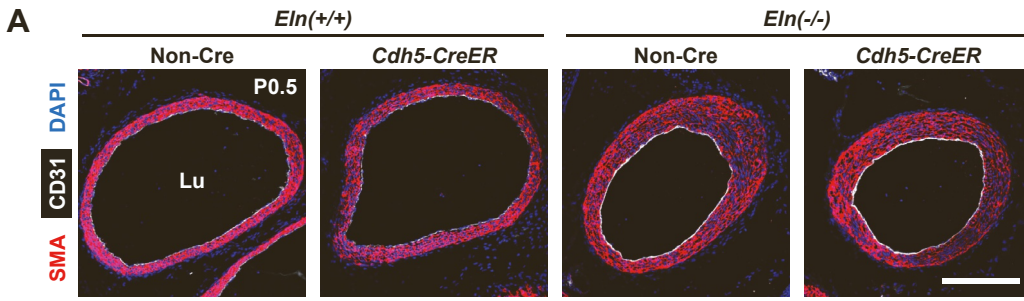


Figure S7. On the *Eln*(-/-), *Psen2*(-/-) background, EC-specific *Psen1* deletion does not attenuate hypermuscularization and stenosis, Related to Figure 3. Transverse sections of the ascending aorta (cranial position, Fig. S2) from pups of indicated genotype at P0.5 were analyzed. **(A)** Sections were stained for SMA, CD31, and nuclei (DAPI). **(B)** Histograms represent aortic medial wall thickness, medial area and lumen area from sections as shown in **A**. n=10 mice. **(C-E)** Sections were stained for SMA, nuclei (DAPI), and either PSEN1 in **C**, HES1 in **D**, or Ki67 in **E**. **(F)** Histogram represents percent of SMCs that are Ki67⁺ in sections as in **E**. n=10-12 mice. Lu, lumen. ns, not significant. **** $P < 0.0001$ by multifactor ANOVA with Tukey's *post hoc* test. Data are presented as mean \pm SD. Scale bars, 200 μ m (**A**) and 40 μ m (**C-E**).

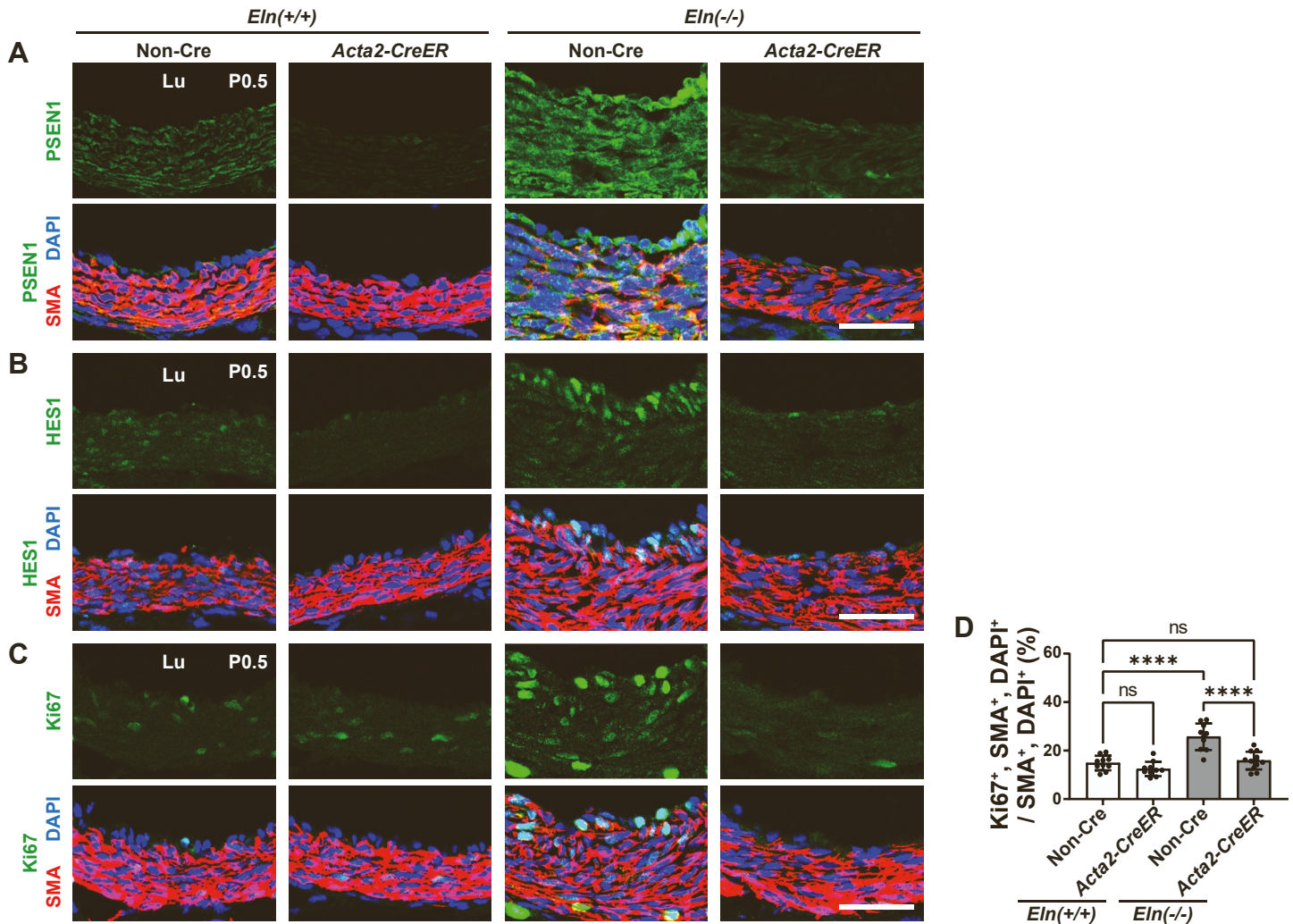


Figure S8. On the *Eln(-/-), Psen2(-/-)* background, SMC-specific *Psen1* deletion reduces HES1 expression and SMC proliferation, Related to Figure 3. Transverse sections of the ascending aorta (cranial position, Fig. S2) from pups at P0.5 of indicated genotype were analyzed. (A-C) Sections were stained for SMA, nuclei (DAPI), and either PSEN1 in A, HES1 in B, or Ki67 in C. (D) Histograms represent percent of SMCs that are Ki67⁺ in sections represented by C. n=10-12 mice. Lu, lumen. ns, not significant. *****P* < 0.0001 by multifactor ANOVA with Tukey's *post hoc* test. Data are presented as mean ± SD. Scale bars, 40 μm (A-C).

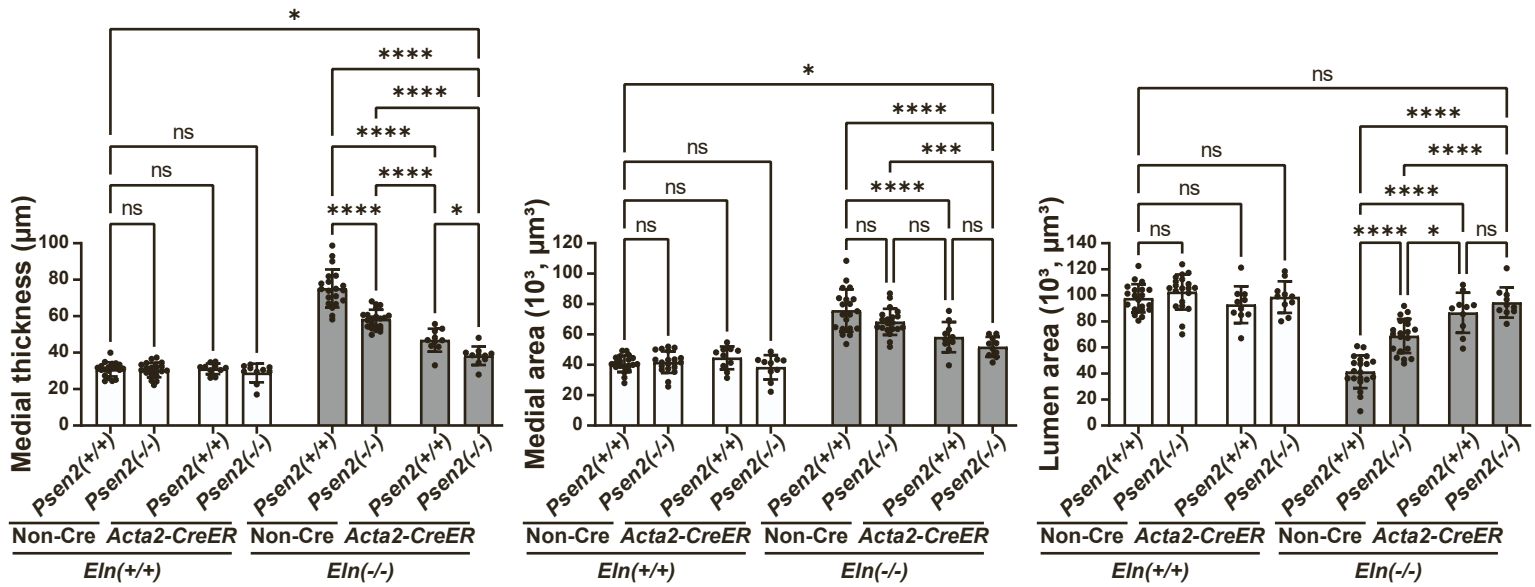


Figure S9. Combined deletion of *Psen1* in SMCs and *Psen2* globally has additional rescue effect on ascending aorta morphology in *Eln*(-/-) mice, Related to Figures 1-3. Histograms demonstrate combined data of ascending aorta medial wall thickness, medial area and lumen area from Figures 1B, 2B, and 3B. n=10-20 mice. ns, not significant. * $P < 0.05$, *** $P < 0.001$, **** $P < 0.0001$ by multifactor ANOVA with Tukey's *post hoc* test. Data are presented as mean \pm SD.

Psen1 (flox/flox)

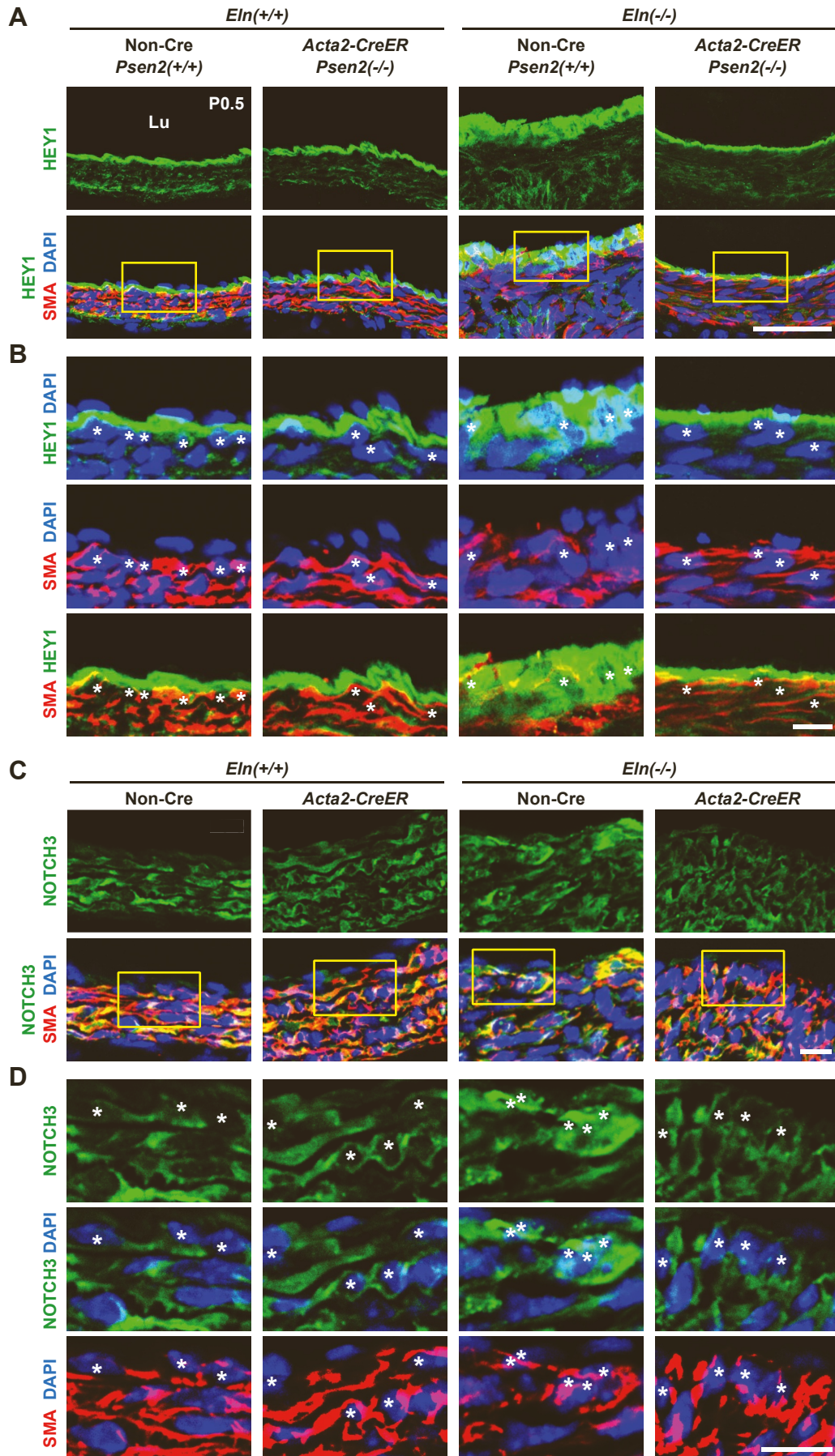


Figure S10. Compound deletion of SMC-specific *Psen1* and global *Psen2* reduces HEY1 and NICD3 expression in inner SMC layers of *Eln*(*-/-*) ascending aorta, Related to Figure 3.

Transverse sections of the ascending aorta (cranial position, Fig. S2) from pups at P0.5 of indicated genotype were analyzed. Sections were stained for SMA, nuclei (DAPI), and either HEY1 in **A-B**, or NOTCH3 in **C-D**. Asterisks indicate nuclei in the inner SMC layers. n=4 mice. Lu, lumen. Scale bars, 50 μm (**A**), 20 μm (**B**) and 10 μm (**C, D**).

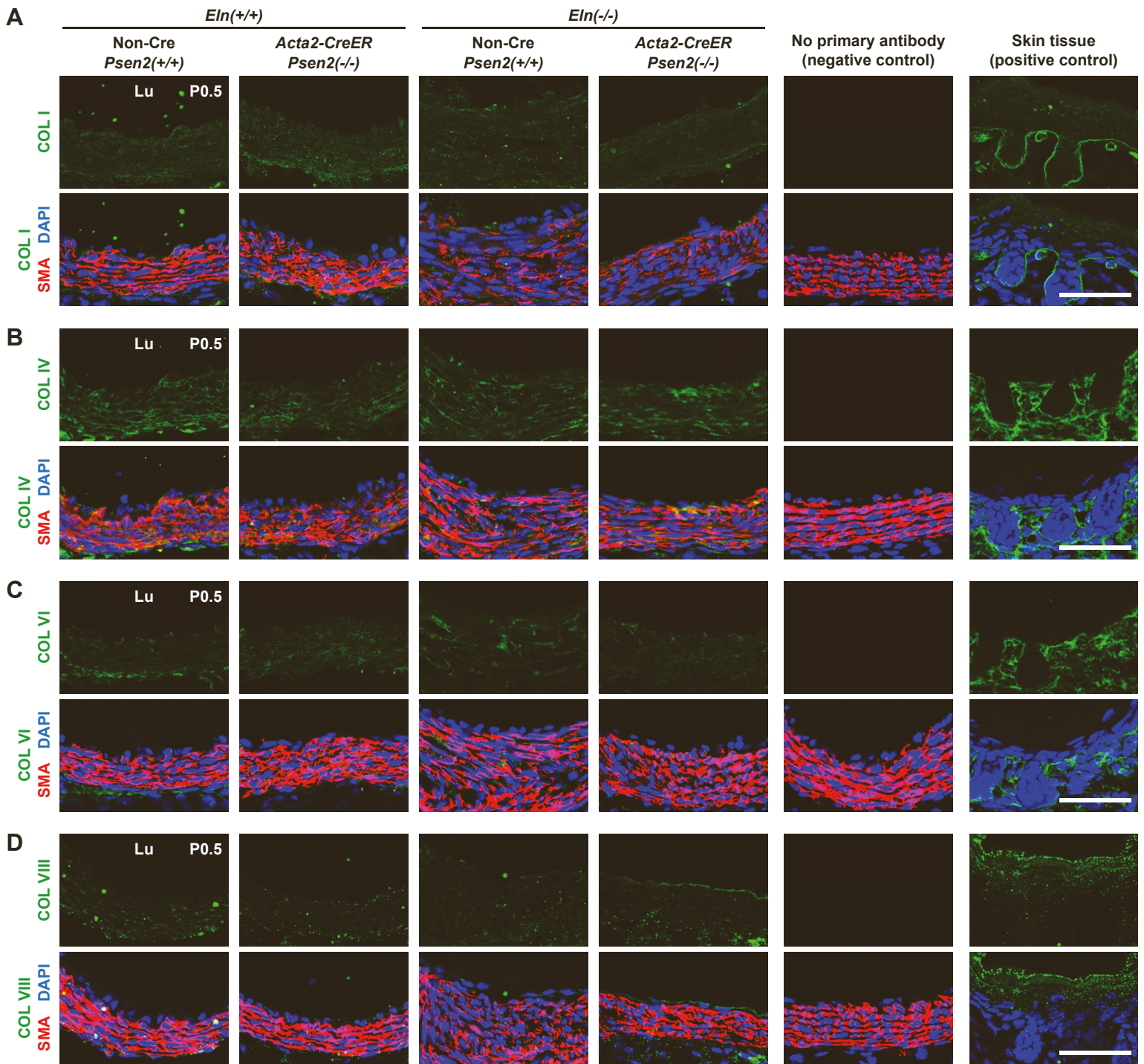


Figure S11. Expression of collagens I, IV, VI, and VIII is not altered by a combination of SMC-specific *Psen1* deletion and global *Psen2* deletion, Related to Figure 3. Transverse sections of the ascending aorta (cranial position, Fig. S2) from pups at P0.5 of indicated genotype were stained for SMA, nuclei (DAPI), and either COL I in **A**, COL IV in **B**, COL VI in **C**, or COL VIII in **D**. Lu, lumen. Sections without primary antibodies for collagens were used as negative controls. Skin tissues from *Psen1(flox/flox)*, *Psen2(+/+)*, *Eln(+/+)*, no Cre pups were used as positive controls. n=4 mice. Scale bars, 50 μ m (**A-D**).

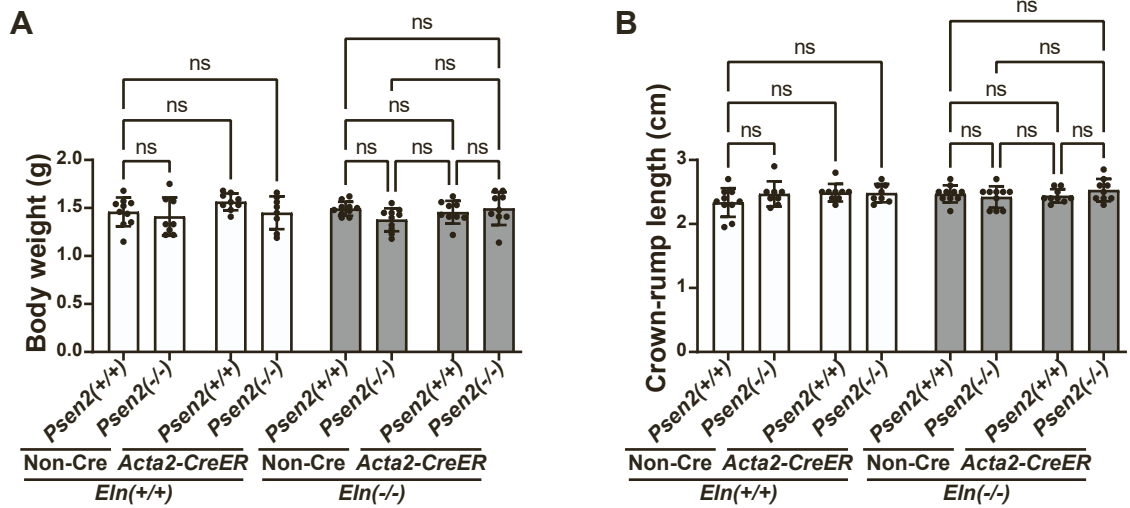


Figure S12. Deletion of *Psen1* in SMCs and/or *Psen2* globally does not alter body size, Related to Figure 3. Histograms represent body weight (A) and crown-rump length (B) of each genotype. n=8-10 mice. ns, not significant. Multifactor ANOVA with Tukey's *post hoc* test was used. Data are presented as mean \pm SD.

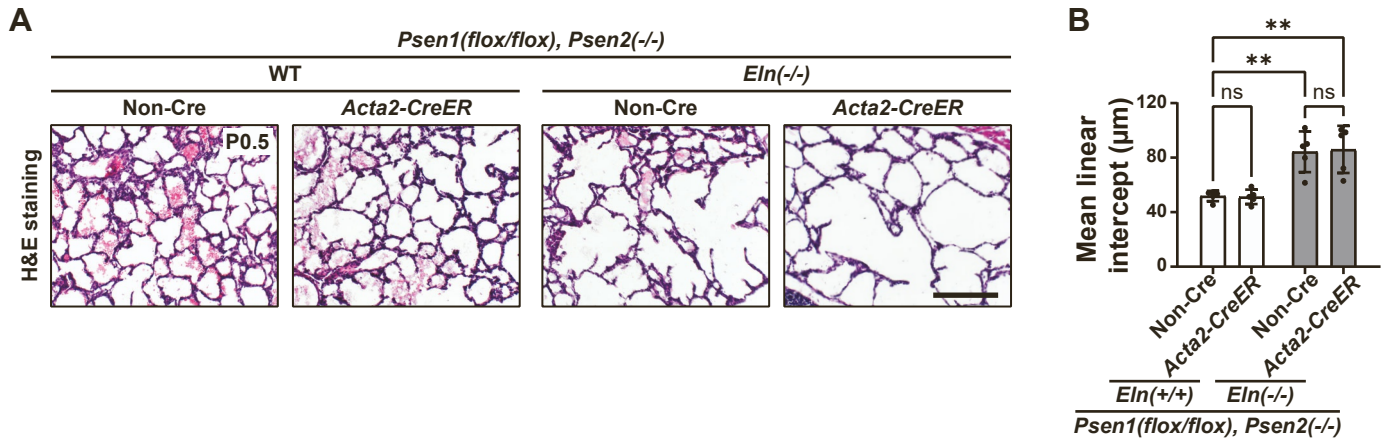


Figure S13. *Psen1* deletion does not improve emphysema in *Eln*(-/-) neonates, Related to Figure 3. (A) Lung transverse sections from indicated genotype at P0.5 were subjected to H&E staining. Scale bar, 200 µm. **(B)** Histograms represent mean linear intercept from sections as shown in A. n=5 mice. ns, not significant. ** $P < 0.01$ by multifactor ANOVA with Tukey's *post hoc* test. Data are presented as mean \pm SD.

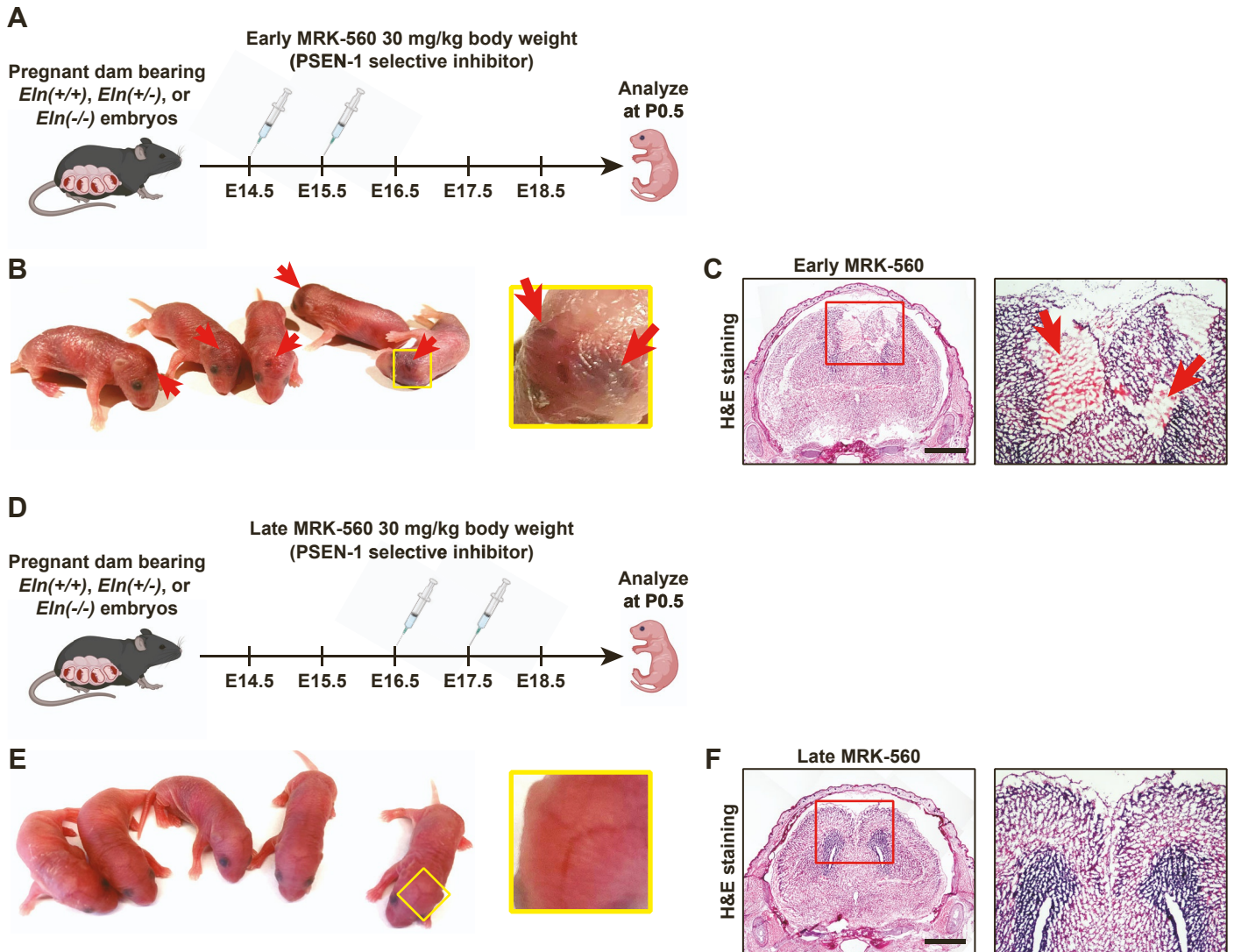


Figure S14. Daily MRK-560 administration on E14.5-15.5, but not E16.5-17.5, induces intracranial hemorrhage in neonates, Related to Figure 5. Pregnant dams bearing *Eln*(+/+), *Eln*(+/-) or *Eln*(-/-) embryos were injected with PSEN-1 selective inhibitor MRK-560 on either E14.5 and E15.5 (**A-C**) or E16.5 and E17.5 (**D-F**). Pups were harvested at P0.5. (**A, D**) Schematic of each experimental schedule. (**B, E**) Gross appearance of pups at P0.5 is shown. Magnified images of the head are shown in the right yellow boxes. (**C, F**) Brain coronal sections were subjected to H&E staining. Right images are the magnification of the red boxes. Arrows indicate intracranial hemorrhage in **B, C**. Scale bars, 1 mm (**C, F**).

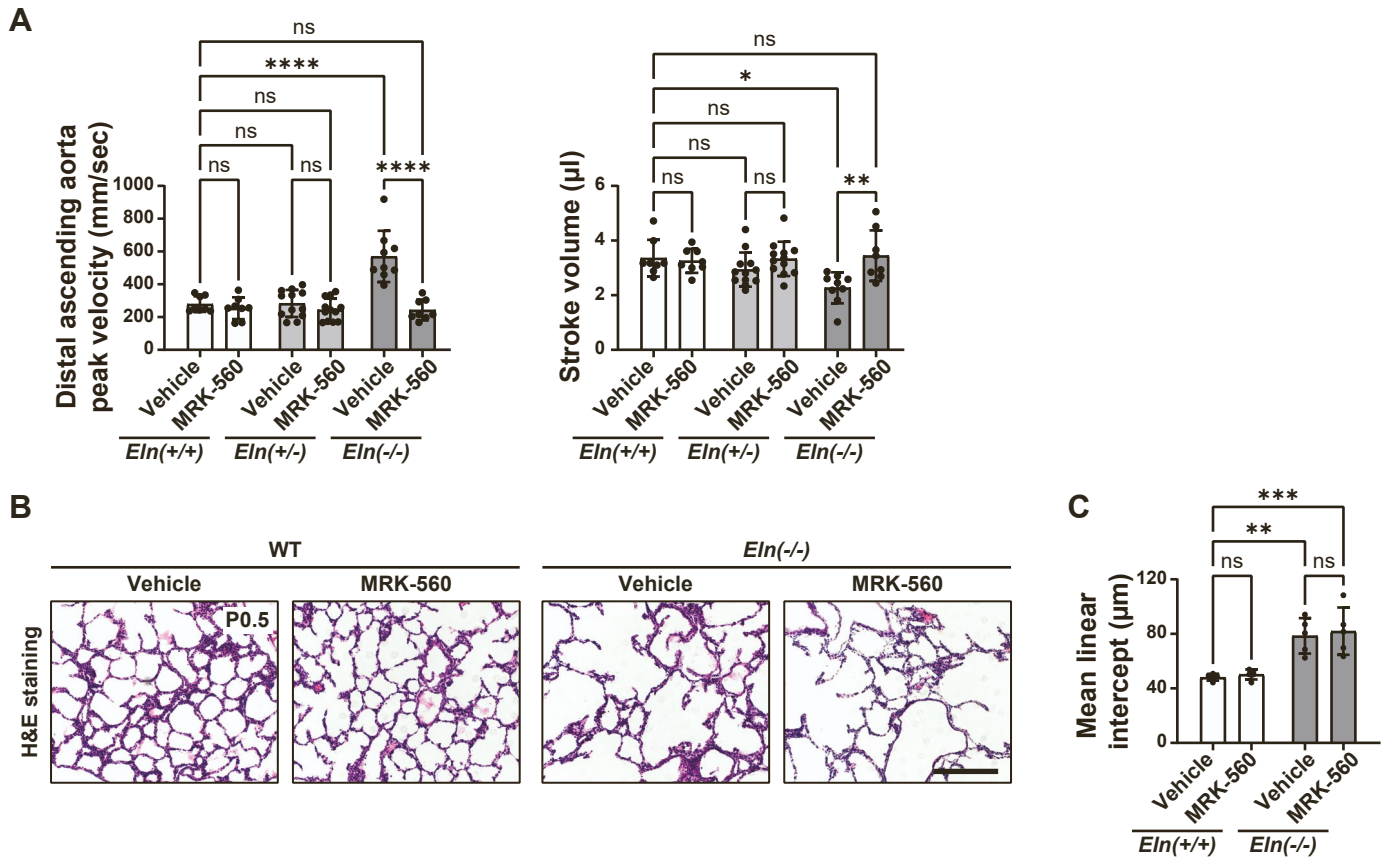


Figure S15. Prenatal MRK-560 treatment improves hemodynamics but not emphysema of *Eln*(*-/-*) pups, Related to Figure 5. Pregnant dams bearing *Eln*(+/+), *Eln*(+/-) or *Eln*(*-/-*) embryos were injected on E16.5 and E17.5 with either vehicle or PSEN-1 selective inhibitor MRK-560, and pups were analyzed at P0.5. **(A)** Pups were subjected to echocardiography. Ascending aorta peak velocity (cranial position, Fig. S2) and cardiac stroke volume were measured by echocardiography. $n=8-12$ mice. **(B)** Lung transverse sections from indicated genotype and/or treatment were subjected to H&E staining. Scale bar, 200 μm . **(C)** Histogram represents mean linear intercept from sections as shown in **B**. $n=5$ mice. ns, not significant. $*P < 0.05$, $**P < 0.01$, $***P < 0.001$, $****P < 0.0001$ by multifactor ANOVA with Tukey's *post hoc* test. Data are presented as mean \pm SD.

Table S1. Primer sequences used for genotyping, Related to STAR Methods.

Gene	Primers
<i>Eln</i>	Primer 1: GGTTG TTCAGACTACAATCTGACC Primer 2: CAACTTTGCCCAAATGACTCTCC Primer 3: GAGAGGTATAGAGGGAAGACTTGCT
<i>Psen1</i>	Primer 1: GGTTTCCCTCCATCTTGGTTG Primer 2: TCAACTCCTCCAGAGTCAGG Primer 3: TGCCCCCTCTCCATTTTCTC
<i>Psen2</i>	Primer 1: CATCTACACGCCCTTCACGG Primer 2: CACACAGAGAGGCTCAAGATC Primer 3: AAGGGCCAGCTCATTCTCC
<i>Cre</i>	Primer 1: GTGGCAGATGGCGCGCGGCAACACCATT Primer 2: GCCTGCATTACCGGTCGATGCAACGA

Table S2. Primer pair sequences used for quantitative reverse transcription polymerase chain reactions, Related to STAR Methods.

Species	Gene	Forward primer	Reverse primer
Mouse	Eln	TTGCTGATCCTCTTGCTCAAC	GCCCCTGGATAATAGACTCCAC
Mouse	Psen1	GGTGGCTGTTTTATGTCCCAA	CAACCACACCATTGTTGAGGA
Mouse	Psen2	GAAGACTCCTACGACAGTTTTGG	CACCAGGACGCTGTAGAAGAT
Mouse	Gapdh	CATCACTGCCACCCAGAAGACTG	ATGCCAGTGAGCTTCCCGTTCAG
Mouse	18S rRNA	CGCCGCTAGAGGTGAAATTC	TTGGCAAATGCTTTTCGCTC
Human	ELN	GTCGCAGGTGTCCCTAGTGT	GGTCCCCACTCCGTA CTTG
Human	PSEN1	TGCACCGTTGTCCTACTTCC	GCTCCTGCCGTTCTCTATTG
Human	PSEN2	AATGAGCCCATATTCCTGCC	TCTTCTCCATCTCCGGGTCG
Human	18S rRNA	TAACGAACGAGACTCTGGCAT	CGGACATCTAAGGGCATCACAG

Supplemental Reference

1. Kang, J., and Shen, J. (2020). Cell-autonomous role of Presenilin in age-dependent survival of cortical interneurons. *Mol Neurodegener* 15, 72. [10.1186/s13024-020-00419-y](https://doi.org/10.1186/s13024-020-00419-y).